Available online at www.sciencedirect.com
SCIENCE DIRECT®
Journal of Solid State Chemistry 178 (2005) 3366–3375
JOURNAL OF SOLID STATE CHEMISTRY
www.elsevier.com/locate/jssc

Diffusion paths formation for Cu^+ ions in superionic Cu_6PS_5I single crystals studied in terms of structural phase transition

A. Gągor[a,*], A. Pietraszko[a], D. Kaynts[b]

[a] W. Trzebiatowski Institute of Low Temperature and Structure Research, Polish Academy of Sciences, P.O. box 937, 50-204 Wroclaw, Poland
[b] Uzhhorod State University, Uzhhorod, Ukraine

Received 13 June 2005; received in revised form 20 August 2005; accepted 23 August 2005
Available online 30 September 2005

Abstract

In order to understand the structural transformations leading to high ionic conductivity of Cu^+ ions in Cu_6PS_5I argyrodite compound, the detailed structure analysis based on single-crystal X-ray diffraction has been performed. Below the phase transition at $T_c = (144-169)$ K Cu_6PS_5I belongs to monoclinic, ferroelastic phase (space group *Cc*) with ordered copper sublattice. Above T_c delocalization of copper ions begins and crystal changes the symmetry to cubic superstructure with space group *F*-43*c* ($a' = 19.528$ Å, $z = 32$). Finally, above $T_1 = 274$ K increasing disordering of the Cu^+ ions heightens the symmetry to *F*-43*m* ($a = 9.794$ Å, $z = 4$). In this work, the final structural model of two cubic phases is presented including the detailed temperature evolution of positions and site occupation factors of copper ions ($R_1 = 0.0397$ for *F*-43*c* phase, and 0.0245 for *F*-43*m* phase). Possible diffusion paths for the copper ions are represented by means of the atomic displacement factors and split model. The structural results coincide well with the previously reported non-Arrhenius behavior of conductivity and indicate significant change in conduction mechanism.

Keywords: Fast-ion conductors; Structural phase transitions; X-ray diffraction; Argyrodites

1. Introduction

Cu_6PS_5I belongs to a large family of solids named after the natural mineral argyrodite Ag_8GeS_6. In the argyrodite family described by the general formula $A^{m+}_{(12-n-y)/m}B^{n+}X^{2-}_{6-y}Y^{-}_{y}$ ($A = Ag^+$, Cu^+, Cd^{+2}, etc.; $B = Ga^{+3}$, Si^{4+}, Ge^{4+}, P^{5+}, etc.; $X = S$, Se, Te; $Y = Cl$, Br, I), several crystals with high ionic mobility have been discovered [1–5]. Argyrodites containing Cu^+ and Ag^+ meet all the structural requirements for this effect.

This work presents the results concerning structural analysis of Cu_6PS_5I single crystals which reveal interesting, mixed ionic–electronic conduction properties. Since there are many potential applications of compounds with high ionic conduction properties, the knowledge of structural transformations to phases characterized by high ionic conductivity remains very important in understanding the structural conditions supporting high mobility of ions in solids at the atomic level.

Despite the fact that numerous papers related to optical, electrical and thermodynamical properties of Cu_6PS_5I have been published so far [6–17], there is still lack of data regarding the low temperature structures and polymorphic phase transitions (PTs). Furthermore, there is a strong divergence between the results concerning thermodynamic properties of samples investigated by different research groups. It manifests in various temperatures of ferroelastic (T_c) and superionic (T_s) PTs. For example, according to Studenyak et al. [6] at low temperature two PTs are observed, a first-order superionic PT $T_s = (165-175)$ K and second-order, ferroelastic one at $T_c = 269$ K; while Girnyk et al. [7] report T_s at 210 K and T_c at 180 K. Finally, second-order PT at 270 K based on the heat capacity measurements was reported by another research group [8].

It was reported in [16] that different preparation procedures in single-crystal growth of Cu_6PS_5I lead to static structural disorder due to the deviation of the copper

*Corresponding author. Fax: +48 71 344 1029.
E-mail address: a.gagor@int.pan.wroc.pl (A. Gągor).

0022-4596/$ - see front matter © 2005 Elsevier Inc. All rights reserved.
doi:10.1016/j.jssc.2005.08.015

content from stoichiometry. This has an influence on the temperature of superionic PT, which varies in the range of 144–169 K for different samples. However, in our previous work [18], we showed that in Cu_6PS_5I crystals temperature of the superionic PT is at the same time the temperature of ferroelastic PT T_c. Moreover, the temperature of this transition also depends on copper content in the sample.

As far as conduction is concerned, conductivity measurements, which were performed on powder samples, show Arrhenius-like behavior above 270 K [1,9]. At room temperature, conduction is purely ionic. An electronic contribution to the total conductivity increases at higher temperatures and above 423 K becomes equal to ionic. The strong anomaly with broad and continuous change in activation energy at 270 K was observed on the Arrhenius plot and much weaker one at around 194 K [9]. Below 270 K, the conductivity demonstrates non-Arrhenius behavior in the range of 80° of temperature.

In this paper, we concentrate only on ionic conductivity. Trying to understand the mechanism for fast-ionic conductivity of Cu^+ ions in Cu_6PS_5I and correlate it with the behavior of the conductivity, we performed a detailed structure analysis based on single-crystal X-ray diffraction.

Recently, we reported a structural PT diagram for this compound based on X-ray diffraction, domain structure observations and calorimetric measurements [18]. The observations under a polarizing microscope did not evidence any domain structure in our samples above $T_c = (144-169)$ K. Below T_c, the crystal belongs to ferroelastic phase with monoclinic symmetry *Cc*. The temperature of T_c depends on the copper content in the sample. Above T_c crystal changes the symmetry to cubic superstructure *F*-43*c* and then at $T_1 = 274$ K to *F*-43*m* system.

In this paper, we focused on two phases, the high temperature *F*-43*m* phase (I) and on the new cubic superstructure *F*-43*c* (II), stable from T_c to T_1. In the cubic phase I, the copper ions are disordered, and below T_1, in the range of cubic phase II, the process of copper ordering takes place. The final structural model of two cubic phases is given including the detailed temperature evolution of positions and site occupation factors of copper ions. Possible diffusion paths for the copper ions are revealed by atomic displacement factors and split model. A comparison of the structural data with non-Arrhenius behavior of conductivity [9] indicates changes in conduction mechanism with temperature increasing: from hopping to mixed hopping and liquid-like behavior.

2. Experimental

The Cu_6PS_5I single crystals were obtained by the conventional vapor transport method [16] at the Uzhhorod State University. Integrated X-ray intensities were measured on Kuma Difraction KM-4 diffractometer equipped with a CCD detector, using graphite monochromated Mo $K\alpha$ radiation. A spherical crystal of 0.25 mm in diameter was prepared in an air mill in order to minimize the influence of the shape on the absorption effect. Accordingly, absorption correction for sphere was applied to integrated intensities. Measurements were carried out at several temperatures between 150 and 500 K. Low temperature was maintained with a nitrogen-gas-flow cooling system (Oxford Cryosystem Controller), $\Delta T = 0.3$ K. The Crys. Alis. software version 1.170.32 (Oxford Diffraction) was used for the data processing and reciprocal space reconstruction. Diffraction data were collected at 165, 235, 295, 425 and 500 K. Table 1 summarizes the crystallographic details derived at 165, 235, 295 and 500 K. Further details of the crystal structure investigations at all temperatures can be obtained from the Fachinformationszentrum Karlsruhe, 76344 Eggenstein-Leopoldshafen, Germany (fax: +49 7247 808 666; e-mail: crysdata@fiz.karlsruhe.de) on quoting the depository numbers CSD 4115486 (500 K), 415487 (420 K), 415488 (295 K) and 415489 (165 K).

The crystal structure at both phases was solved by direct methods using SHELXS97 program package. The least-squares structure refinement was performed on the program package JANA2000 [19]. The appropriate occupancies for copper positions were refined using isotropic model in order to avoid bias resulting from correlations between occupancy and anisotropic thermal components U_{ij}.

Our research was based on two samples with different copper contents. Sample I which was used in data collection for structure refinement was grown with copper deficiency, which resulted in decreased temperature of the ferroelastic PT $T_c = 144$ K. The room temperature refinement of copper occupancy factors gave following formula $Cu_{5.83}PS_5I$. The summary copper content acquired at room temperature was fixed in refinements at low temperature. The final refined atomic coordinates and displacement parameters are given in Tables 2–5.

The lattice parameters were determined by Bond [20] procedure on a Bond diffractometer using graphite monochromated Cu $K\alpha$ radiation. The second sample, which was used in this experiment, was grown with higher copper content than the sample used in data collection. Its ferroelastic transition temperature was found to $T_c = 165$ K. The accuracy of the lattice parameter determination $\Delta a/a$ was 1×10^{-4} in the cubic phase and 9×10^{-4} in the monoclinic phase, due to broadening of Bragg peaks connected with twinning of the crystal.

3. Results and discussion

3.1. Cubic phase I

The crystal structure of Cu_6PS_5I room temperature phase belongs to cubic symmetry with space group *F*-43*m* ($a = 9.7940(1)$), which is characteristic for high temperature argyrodite form. The rigid $[PS_5I]$ framework accommodates 24 copper ions among 72 permissible positions. Copper atoms are located statistically at the edge of SI_4 tetrahedron occupying the 24*g* and 48*h* Wyckoff positions, with site occupation factors 0.465 and 0.254, respectively.

Table 1
Experimental details

Crystal data				
Formula	$Cu_{5.83}PS_5I$	$Cu_{5.83}PS_5I$	$Cu_{5.83}PS_5I$	$Cu_{5.83}PS_5I$
Temperature (K)	165	235	295	500
Crystal system, space group	Cubic, *F*-43*c*	Cubic, *F*-43*c*	Cubic, *F*-43*m*	Cubic, *F*-43*m*
Z, Pearson code	32, cF560	32, cF560	4, cF52	4, cF52
Unit cell dimensions (Å)	19.5033(1)	19.5275(1)	9.7940(1)	9.8130(1)
Volume ($Å^3$)	7418.6	7446.3	939.5	944.9
Formula weight	688.7	688.7	688.7	688.7
Calculated density (g/cm^3)	4.93	4.92	4.88	4.84
Data collection				
Radiation type/wavelength (Å)	Mo $K\alpha$/0.71069	Mo $K\alpha$/0.71069	Mo $K\alpha$/0.71069	Mo $K\alpha$/0.71069
2θ range for data collection (deg.)	92.5	92.51	92.28	92.20
Limiting indices	$-25<h<36$	$-27<h<27$	$-16<h<19$	$-19<h<12$
	$-32<k<39$	$0<k<28$	$-19<k<12$	$-12<k<19$
	$-38<l<26$	$2<l<38$	$-15<l<19$	$-19<l<16$
Criterion for observed reflections	$I>3\sigma(I)$	$I>2\sigma(I)$	$I>3\sigma(I)$	$I>3\sigma(I)$
No. of reflections collected/unic	27,799/2248	4882/2571	4387/436	3999/357
R_{int}	0.048	0.0393	0.032	0.1158
Refinement				
Refinement on	*F*	F^2	*F*	*F*
Program used	JANA2000	SHELXL97	JANA2000	JANA2000
Data/parameters	2248/50	2571/32	436/18	357/17
S_{all}	1.38	0.80	1.29	1.24
Final R_{obs}, Rw_{obs}	0.0393, 0.0448	0.0329, 0.0848	0.0245, 0.0328	0.0522, 0.0520
Final R_{all}, Rw_{all}	0.0621, 0.0568	0.1348	0.0260, 0.0336	0.0688, 0.0614
Extinction method	B–C type 1 Gaussian isotropic	SHELXL97	B–C type 1 Gaussian isotropic	B–C type 1 Gaussian isotropic
Extinction coefficient	0.0234(15)	0.000156(2)	0.0249(16)	0.0244(18)

Table 2
Wyckoff positions, site symmetry, fractional atomic coordinates, isotropic displacement parameters ($Å^2$) and site occupation factors for Cu_6PS_5I (*F*-43*m*, $T = 295$ K)

Atom	Wyckoff position	Site symmetry	*x*	*y*	*z*	U_{iso}	S_{of}
I	4*a*	−43*m*	0	0	0	0.01515(6)	1
P	4*b*	−43*m*	0	0	0.5	0.00734(11)	1
S1	4*d*	−43*m*	0.25	0.25	0.75	0.01502(14)	1
S2	16*e*	.3*m*	0.37869(5)	0.37869(5)	0.37869(5)	0.01077(8)	1
Cu1	24*g*	2.*mm*	0.25	0.25	0.97671(17)	0.0371(5)	0.465
Cu2	48*h*	..*m*	0.2034(2)	0.2966(2)	0.51951(19)	0.0277(4)	0.254

Table 3
Wyckoff positions, site symmetry, fractional atomic coordinates, isotropic displacement parameters ($Å^2$) and site occupation factors for Cu_6PS_5I (*F*-43*c*, $T = 165$ K)

Atom	Wyckoff position	Site symmetry	*x*	*y*	*z*	U_{iso}	S_{of}
I1	8*a*	23.	0	0	0	0.01111(8)	1
I2	24*c*	−4..	0.25	0.25	0	0.00724(7)	1
P1	8*b*	23.	0.25	0.25	0.25	0.0070(3)	1
P2	24*d*	−4..	0.25	0	0	0.0034(2)	1
S	32*e*	.3.	0.12639(4)	0.12639(4)	0.12639(4)	0.00880(13)	1
S1	96*h*	1	0.31094(4)	0.06238(4)	0.05888(4)	0.00648(16)	1
S2	32*e*	.3.	0.31096(4)	0.18904(4)	0.18904(4)	0.00508(11)	1
Cu1	96*h*	1	0.12872(6)	0.12466(6)	0.01264(6)	0.0374(4)	0.7689
Cu2	96*h*	1	0.10060(17)	0.10003(17)	0.01230(18)	0.0159(7)	0.2048
Cu4	96*h*	1	0.24032(4)	0.14528(4)	0.10406(4)	0.02846(17)	0.9683

Table 4
Anisotropic displacement parameters U_{ij} (Å^2) for Cu_6PS_5I (F-43m)

Atom	U_{11}	U_{22}	U_{33}	U_{12}	U_{13}	U_{23}
$T = 295$ K						
Cu1	0.0471(9)	0.0471(9)	0.0172(5)	0.0308(12)	0	0
Cu2	0.0310(6)	0.0310(6)	0.0211(8)	−0.0150(7)	0.0000(4)	0.0000(4)
$T = 500$ K						
Cu1	0.0438(11)	0.0438(11)	0.0273(14)	0.003(2)	0	0
Cu2	0.0425(13)	0.0425(13)	0.030(2)	−0.0141(16)	−0.0047(12)	0.0047(12)
Cu3	0.027911	0.027911	0.027911	0.01209	−0.01209	0.01209

Table 5
Anisotropic displacement parameters U_{ij} (Å^2) for Cu_6PS_5I (F-43c, $T = 165$ K)

Atom	U_{11}	U_{22}	U_{33}	U_{12}	U_{13}	U_{23}
Cu1	0.0513(8)	0.0538(8)	0.0072(3)	0.0476(7)	0.0012(4)	0.0004(4)
Cu2	0.0145(12)	0.0134(11)	0.0197(13)	0.0055(9)	0.0032(9)	0.0006(8)
Cu4	0.0105(2)	0.0424(3)	0.0324(3)	0.0019(2)	−0.0022(2)	−0.0269(3)

The 24-fold Cu1 position is triangularly coordinated by S atoms (one S1 and two S2). The distances Cu1–S1 of 2.22 Å and Cu1–S2 of 2.28 Å correlate well with the value of 2.28 Å calculated in Cu_2S for triangular coordination of copper [21]. However, triangular coordination is slightly deformed and Cu1 position is shifted from the center toward S1 position. The 48-fold Cu2 position is tetrahedrally coordinated by S and I atoms (one S1, one I and two S2) (Fig. 1a). The average Cu2–S distance of 2.34 Å compares reasonably well with the value of 2.28 Å calculated in chalcopiryte $CuFeS_2$ for an ideal tetrahedral coordination [22]. Copper is displaced from the center of the tetrahedron toward the face of the tetrahedron. This distortion gives reasonable Cu–I distance of 2.82 Å.

Because of disorder copper atoms are found to be very close to each other in a unit cell (Cu1–Cu2 of 0.65 Å, Cu2–Cu2 of 1.29 Å). Although these distances do not have physical meaning they give an insight into possible diffusion paths for copper ions.

Phosphorus atoms are surrounded by four sulfur atoms at a characteristic distance of 2.0578(1) Å forming regular tetrahedra. Table 6 gives the bonds lengths of the Cu, P and S environment.

With the temperature increase the largest changes were observed in the copper sublattice. Above 420 K summary occupation of available copper positions decreased. This effect is of interest for the copper conduction. It indicates that a part of copper ions diffuses to new positions in the lattice. Structure refinement at 500 K based on the room temperature model gave acceptable residual factor $R_1 = 5.85$ but the occupation of Cu1 and in principle Cu2 position decreased noticeably (Fig. 2a). Furthermore, difference-Fourier maps revealed the presence of copper atoms at the new 16(e) Wyckoff position. Introduction of this new position in refinement allowed to balance the copper content in the sample and reduced R_1 to 5.62.

Above 500 K electron density of copper ions becomes significantly diffused, which indicates a rise in the disorder in the copper sublattice. To account for this effect we extended the refinement on the anharmonic Gram–Charlier model of temperature components [23]. We adopted a mixed system of refinement. The parameters of the Cu2 displacement factors were refined in the third-order anharmonic approximation:

$$T(\mathbf{h}) = T_{\mathrm{harm}}(\mathbf{h})[1 + (2\pi\mathrm{i})/3!c_{pqr}\mathbf{h}_p\mathbf{h}_q\mathbf{h}_r],$$

where $T_{\mathrm{harm}}(\mathbf{h})$ ($= \exp(-\beta_{pq}\mathbf{h}_p\mathbf{h}_q)$) and β_{pq} are anisotropic harmonic temperature parameters, c_{pqr} are anharmonic temperature parameters of the third order and $\mathbf{h}$ is the scattering vector with components $(h1,h2,h3) = (h,k,l)$. It improved residual factor $R_1 = 5.21$ and reduced the electron residuals on the difference-Fourier maps in vicinity of Cu2 position. For Cu1 and Cu3 atoms anisotropic refinement was applied. The anharmonic refinement of this position did not improve the refinement and was at the expanse of the observation-to-parameter ratio. The projection of the $S1I_4$ tetrahedron and the coordination of copper ions at 500 K is presented in Fig. 3a.

3.2. Cubic phase II

In Cu_6PS_5I compounds, X-ray single-crystal diffraction data confirm a reversible cubic–cubic PT between 270 and 274 K. From the systematic extinction conditions noncentro-symmetric F-43c group has been determined with lattice constant $a = 19.5033(1)$ at 165 K. The changes of atomic parameters versus temperature are presented in Fig. 4. The small distortion of the lattice parameters above

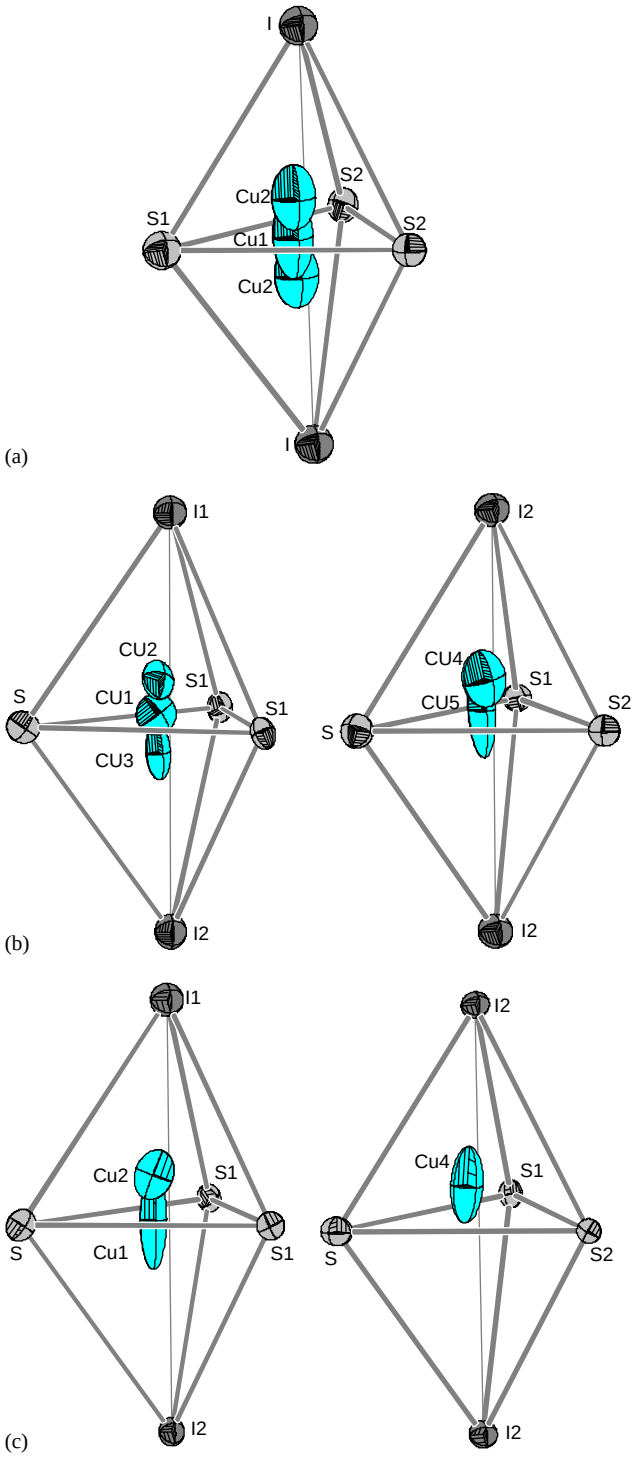

Fig. 1. Coordination of Cu^+ ions in: (a) *F*-43*m* phase, $T = 295$ K; (b) *F*-43*c* phase, $T = 235$ K; and (c) *F*-43*c* phase, $T = 165$ K. After the transition to cubic phase II Cu1 copper ion converts to Cu1 and Cu5, Cu2 converts to Cu2, Cu3 and Cu4.

170 K is associated with the existence of micro-strains connected with the sample mounting on the goniometer, and can be easily reduced after applying appropriate constrains for regular structure to the procedure of lattice constants determination.

The intensity of new phase reflections was very poor below the PT. However, it increased with temperature lowering. It allowed us to measure intensities of quality well enough for structure refinement below 200 K.

As mentioned already above, the PT observed in Cu_6PS_5I implies an ordering process of Cu^+ ions. The framework structure is in principle independent of temperature. The axis doubling is associated with increment of independent crystallographic sites for Cu^+ ions. Namely, the change of the symmetry to *F*-43*c* at phase II provides six independent 96-fold Cu positions with point symmetry C_1 in the rigid skeleton of an anion framework. It provides also two different tetrahedral coordinations for Cu^+ ions: Cu(I1S1S1S) and Cu(I2S1S2S). Further in the text this coordinations are denoted as Cu($I1S_3$) and Cu($I2S_3$), respectively. At 235 K copper ions accommodate five nonequivalent sites which refer to copper sites in Cubic phase I (Fig. 1b). However, copper ions do not locate in one tetrahedral site characteristic for the high temperature phase. It implies ordering process. At 165 K only three copper positions are occupied (Fig. 1c). The Cu1 position is triangularly coordinated by S atoms (S1, S1, S) with average Cu1–S1 distance of 2.28 Å and Cu1–S of 2.22 Å. The Cu1 position is displaced from the center of sulfur triangle toward S position.

The environment for Cu2 position is distorted tetrahedral (I1, S1, S1, S) with average Cu2–S1 distance of 2.36 Å, Cu2–S distance of 2.33 Å and Cu2–I1 distance of 2.79 Å. In comparison with room temperature phase, this position is shifted distinctly from the tetrahedral site toward the SS1I1 tetrahedral face, which leads to one longer Cu2–S1 distance. This tendency in the case of Cu4 position is not observed, although Cu4 is also tetrahedrally coordinated (I2, S1, S2 and S). The shift toward a face of tetrahedron in the case of this position is very slight. The refined distances are as follows: Cu4–S1 of 2.31 Å, Cu4–S2 of 2.32 Å, Cu4–S of 2.29 Å and Cu4–I of 2.88 Å.

In summary, observed structural PT does not provide any significant changes in coordination of copper ions. However, important changes are observed in copper sublattice. With temperature increase copper ions have tendency to occupy two positions with different coordinations: triangular in the case of Cu1 and tetrahedral in the case of Cu4.

The tendency that with temperature lowering copper ions occupy three-fold and four-fold coordinated Cu positions corresponds to the model of Cu arrangement in the monoclinic *Cc* phase proposed in Cu_6PS_5Br compounds [24]. Taking into account the monoclinic low temperature phase of Cu_6PS_5Br three copper atoms occupy the three-fold position and three copper atoms occupy four-fold positions. This ordering of Cu atoms can be at the origin of the last *F*-43*c*–*Cc* PT. The projection of the SI_4 tetrahedron and coordination of copper ions at 165 K is presented in Fig. 3b.

In structure refinement at 165 K, we also adopted mixed system. The possible location of the Cu4 atom was

Table 6
Site coordination and calculated distances (Å) from refinements at 165, 295 and 500 K

165 K		295 K		500 K	
Atom P1		Atom P		Atom P	
4 × S2	2.0568(8)	4 × S2	2.0578(5)	4 × S2	2.0515(15)
Atom P2					
4 × S1	2.0529(8)				
Atom S		Atom S1		Atom S1	
3 × Cu1	2.2205(12)	6 × Cu1	2.2204(16)	6 × Cu1	2.230(4)
3 × Cu2	2.334(4)	12 × Cu2	2.3478(19)	12 × Cu2	2.342(5)
2 × Cu4	2.2905(15)			4 × Cu3	2.1296
Atom Cu1		Atom Cu1		Atom Cu1	
S1	2.2725(13)	2 × S2	2.2766(11)	2 × S2	2.281(3)
S1	2.2793(13)	2 × Cu2	0.646(2)	2 × Cu2	0.648(4)
Cu2	0.724(4)	4 × Cu2	2.901(2)	4 × Cu2	2.901(5)
Cu2	2.888(4)			2 × Cu3	2.0060(19)
Cu2	2.844(4)				
Cu4	2.8346(19)				
Atom Cu2		Atom Cu2		Atom Cu2	
S1	2.396(4)	2 × S2	2.344(2)	2 × S2	2.359(4)
S1	2.338(4)	Cu1	0.646(2)	Cu1	0.648(4)
Cu1	0.724(4)	2 × Cu1	2.901(2)	2 × Cu1	2.901(5)
Cu1	2.844(4)	Cu2	1.290(3)	Cu2	1.295(5)
2 × Cu1	2.888(4)	2 × Cu2	2.548(3)	2 × Cu2	2.535(6)
2 × Cu2	2.438(5)			Cu3	1.494(4)
				Cu3	2.595(4)
Atom Cu4				Atom Cu3	
S1	2.309(2)			3 × Cu1	2.0060(19)
S2	2.3193(19)			3 × Cu2	1.494(4)
Cu1	2.8346(19)			3 × Cu2	2.595(4)

described by the Gram–Charlier model of the displacement parameters. Using this approach with respect to this position we were able reduce the residual factor R_1 by approximately 1% and the difference-Fourier residues. However, Cu1 and Cu2 positions required different descriptions. The structure was better refined with the split-atom model of Cu1 and Cu2 atoms than by one atom with the anharmonic displacement parameters. The data thus obtained were used to construct the joint probability density functions (PDFs) [25].

3.3. Ionic migration

In the cubic phase I, 24 Cu^+ ions partly occupy systems of various tetrahedral, triangular and linear low-coordination sites within an anion framework. They are delocalized in a unique cell on 72 positions below 425 K, and on 88 positions in higher temperatures. Moreover, it has been demonstrated that low energy barriers separate this two-, three- and four-fold coordination of copper in solid halides and chalcogenides [26]. This provides favorable means for ionic migration.

In high temperature Cu_6PS_5I phase as well as in γ-Cu_7PSe_6 [27], three copper positions participate in the diffusion. Thermally active mobile copper ions move to vacant neighboring sites from the occupied sites along the conduction path. At room temperature the Cu atoms make strongly anharmonic vibrations along the edge of $S1I_4$ tetrahedra and are able to overcome the rather flat potential barrier to the neighboring lattice site. Moreover, the two Cu1 and Cu2 PDFs strongly overlap (see Fig. 2a), which confirms a possible movement of copper between these two positions. Taking into account the relatively close vicinity of these two positions it appears probable that jumps of Cu ions between them are easily thermally activated.

Above 425 K copper adopts the low, linear I–S coordination that creates the conducting 'bridge' between Cu2 and Cu2 positions (Fig. 5). The appearance of this new copper position leads to an emergence of a pseudo-cluster centered at S1 and reveals possible copper diffusion paths for copper migration within $S1I_4$ tetrahedra. The Cu3–S/I average distance of 2.12 Å found in the linear Cu(SI) configuration is comparable to that calculated in γ-Cu_7PSe_6 (2.19 Å), although in Cu_6PS_5I crystal atomic displacement factors are lower and overlap only in the case of Cu1 and Cu2 atoms. Moreover, there is not a connection between the clusters throughout the structure, which explains lower conductivity of Cu_6PS_5I crystals. The occupation factor of Cu3 site is relatively low compared to Cu1 and Cu2, also its

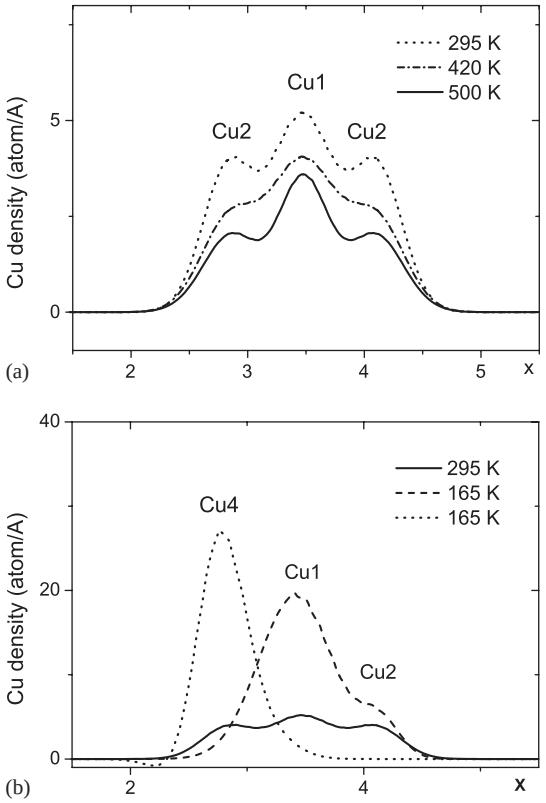

Fig. 2. (a) Probability density distribution of the Cu1 and Cu2 atom along the edge of $S1I_4$ tetrahedron at 295, 420 and 500 K. (b) Probability density distribution of the Cu1, Cu2 and Cu4 atoms along the edge of SI_4 tetrahedron at 295 and 165 K.

PDF is spread over a large area around the three-fold axis. It indicates a short duration of stay of Cu ions on this site during their migration. This observation suggests that Cu3 is not stable in linear configuration and is in agreement with usual observations in chalcogenides [26].

The representation of the joint PDF of iodine and copper ions at 500 K, with Cu3 ion clearly marked is presented in Figs. 5, 6a and b. On the basis of joint PDFs the pseudo-potentials along Cu1–Cu2–Cu3 copper diffusion paths were calculated (see Fig. 6c).

In disordered structures, diffraction data give only the average content of unit cells and PDFs that are the average over the different PDFs of all unit cells. Because of this special average, the potential derived from diffraction experiment does not give the average potential energy of the ions, but it is only pseudo-potential which is broader than the real average potential. However, it is possible in the case of resolved positions to determine the potential difference between symmetrically inequivalent sites which is given by

$$V(x_1) - V(x_2) = -kT \ln[w_1 \mathrm{PDF}_1(x_1)/w_2 \mathrm{PDF}_2(x_2)],$$

where w_1 and w_2 are occupation factors [25].

Analysis of the site potential for copper cations shows that Cu1 has a lower potential than Cu2, and its PDF is more contracted. Low energy barrier $\Delta E = 0.02$ eV between Cu1 and Cu2 sites together with strong overlapped PDFs indicate the fluid-like movement of copper along the edge of $S1I_4$ tetrahedra. From the other side, relatively high energy barrier $\Delta E = 0.28$ eV between Cu2 and Cu3 sites suggests hopping mechanism for diffusion. The energy barrier obtained is of the order of the activation energy (0.35 eV [1] and 0.41 eV [9]) determined from conductivity measurements, although it only contains information about the hopping barrier within tetrahedral clusters. This can explain its lower value compared to the data from conductivity measurements.

An explanation of the migration of Cu ions into neighboring copper clusters may be two-fold. Since the PDF of Cu2 position is rather contracted a very weak widening of PDF toward another Cu2 position (Cu2–Cu2 of 3.01 Å) is observed. Similar copper distribution is observed in γ-Cu_7PSe_6 where there is also lack of connection between the clusters. However, such connections are observed in argyrodites containing mobile silver ions, i.e., γ-Ag_7PSe_6, Ag_7GeSe_5I crystals. The PDFs of this position overlap and give rise to conducting 'bridges' between tetrahedral clusters [28]. This observation confirms lower conductivity of compounds with Cu mobile ions.

There is also another possibility of Cu^+ migration between clusters. It was proposed by Kuhs in Cu_6PS_5Br crystals [29]. It suggests that another 24(*f*) position for Cu ions is available in the lattice. The coordination of this site is triangular (one Br and two S1) with an average distance of 2.17 Å and the closest hopping distance to another copper position of 2.34 Å. However, jumping of Cu ion from one cluster to another via this position is only probable if the P position adjoining new Cu position is not occupied. In the case of Cu_6PS_5I, we were not able to locate any copper in the site discussed above, nor any disorder in P sublattice was observed. Summarizing, the most probable conduction path for copper between the copper clusters is connected with the shortest distance between two Cu2–Cu2 positions. However, we were not able to establish the energy barrier between them because of very contracted character of its PDFs. The hopping between these two positions is probably facilitated by coupled oscillations of anion sublattice.

With temperature lowering the copper cations preferably occupy the most stable tetrahedral and triangular sites along diffusion paths. The unit cell doubles in all dimensions and the symmetry changes to *F*-43*c*. It provides six independent, 96-fold Cu positions with point symmetry C_1 and two different tetrahedral coordinations for Cu^+ ions: $Cu(I1S_3)$ and $Cu(I2S_3)$. The two tendencies in ordering process of the copper sublattice are observed with temperature lowering. The Cu4 tetrahedral site is strongly preferred by Cu^+ ions. With temperature decrease the copper ions shift from planar CuS_3 configuration toward the tetrahedral $Cu(I2S_3)$ site and at 165 K this position is almost fully occupied (Fig. 2b). On the other hand, the ions coordinated by the $Cu(I1S_3)$ tetrahedrons prefer the planar triangular sulfur configuration. The

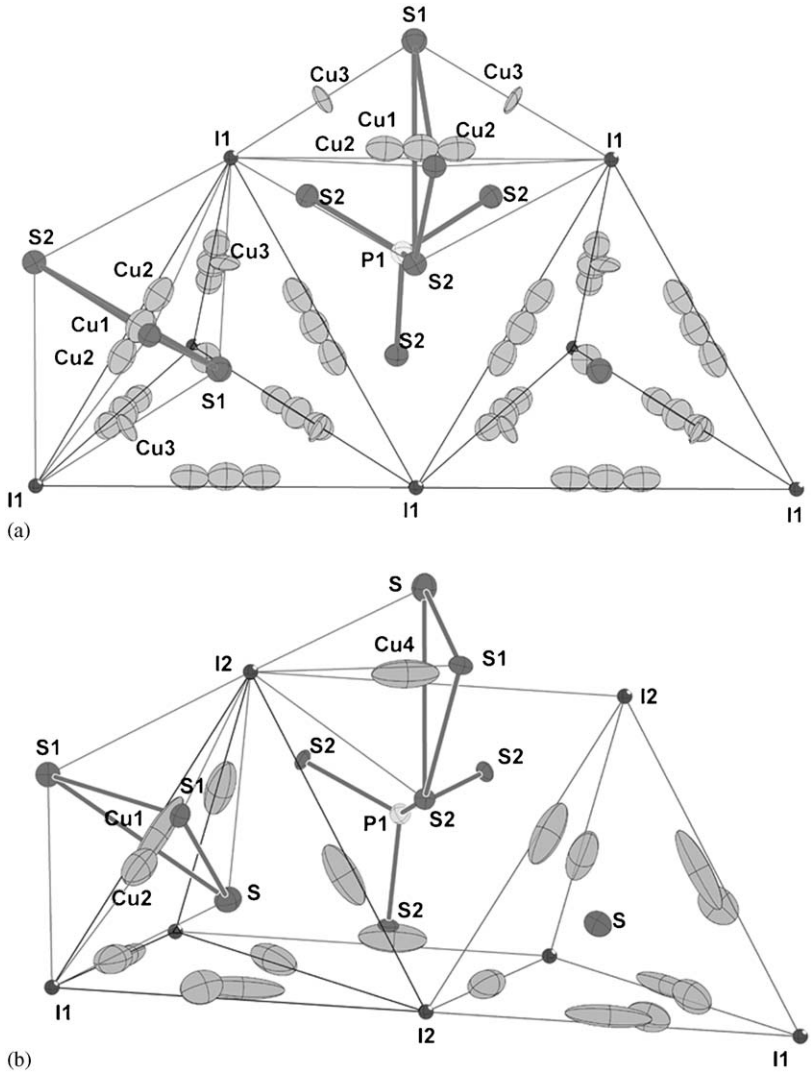

Fig. 3. Coordination system and copper distribution in: (a) cubic phase I (F-43m), $T = 500$ K and (b) cubic phase II (F-43c), $T = 165$ K. Radii of thermal ellipsoids have been reduced for all atoms for clarity of the picture.

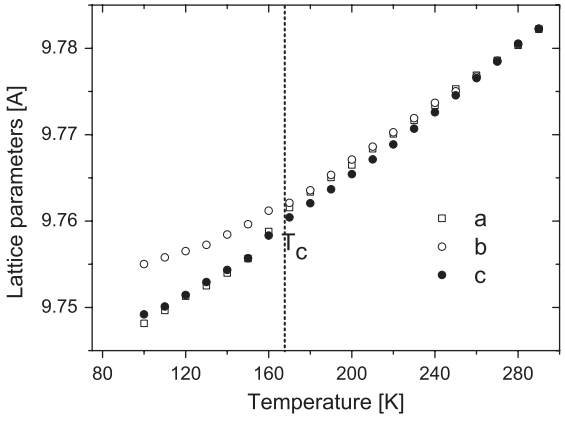

Fig. 4. Temperature dependence of the unit cell parameters a, b and c for Cu_6PS_5I with increased copper content.

occupancy of this site increases with temperature lowering, but even at 165 K the Cu^+ ions are not well localized. The localization of the copper is only partial, which indicates

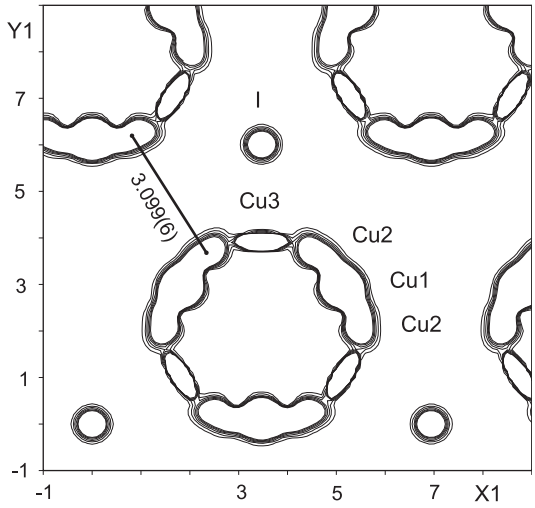

Fig. 5. Joint probability density function map at level 0.1–0.005 $Å^{-3}$, cubic phase I, $T = 500$ K, plane (111). Pseudo-cluster of copper within SI_4 tetrahedron is well pronounced, there is no connection between clusters.

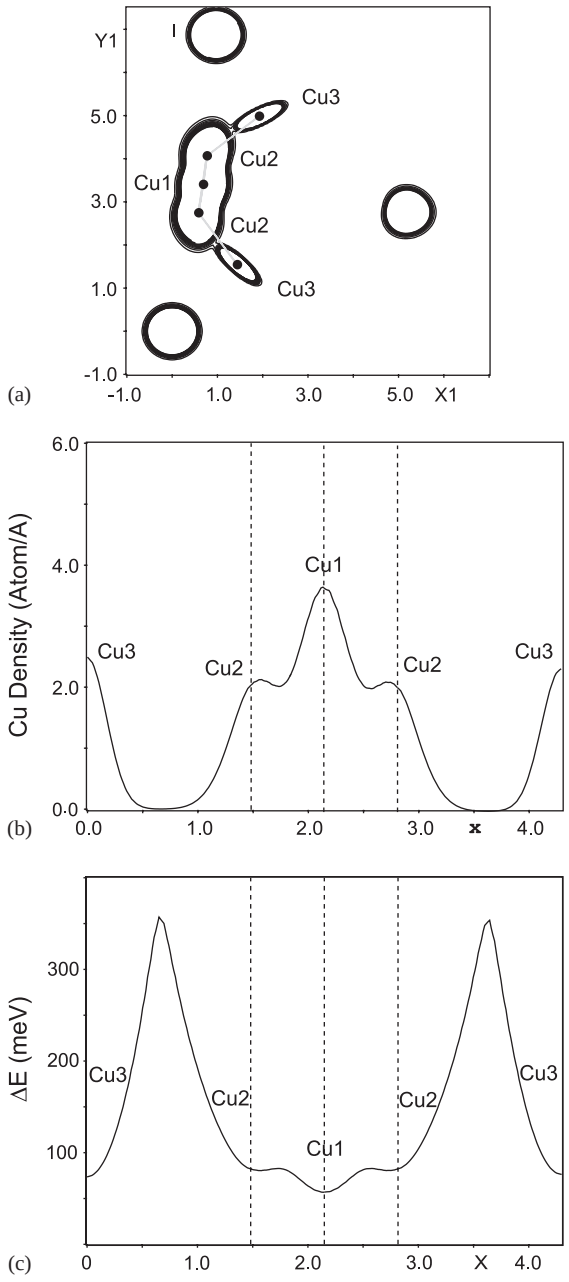

Fig. 6. (a) Joint probability density functions map at levels 0.1–0.005 Å^3, $T = 500$ K, section passing through Cu1, Cu2 and Cu3 positions marked in the picture. (b) Probability density distribution of the Cu1, Cu2 and Cu3 atoms along lines joining the centers of these atoms. (c) Pseudo-potentials within the copper ion-diffusion path.

possible movement of copper between these two positions. It is worth noticing that the displacement factors of I1 in Cu(I1S$_3$) tetrahedron coordinating Cu2 atom are higher than the displacement factors of the I2 atom. It suggests that larger thermal ellipsoids of I1 atoms contrary to I2 result from Cu migration between Cu1 and Cu2 sites and Coulomb interaction between Cu, I and S ions related with this motion.

Despite the fact that with temperature decrease copper atoms have a tendency to localize there still exists an empty site in the lattice with relatively low energy barriers between them. As a result, Cu ions can move from one site to another empty site by tunneling [8]. This can explain the fact that Cu_6PS_5I displays high ionic conduction in F-43c phase even at unusually low temperatures for this process.

4. Conclusions

On the basis of X-ray diffraction on single crystal of Cu_6PS_5I it was established that structural PT at $T_1 = 274$ K and all the changes in the structure of the cubic phases I and II are due to copper migration. Comparing our results with conduction properties of this compound [9] we conclude that the temperature of the electrical PT at 270 K coincide with the temperature T_1. Furthermore, the temperature range of non-Arrhenius behavior of conductivity covers the wide region of cubic phase II. It confirms the important change in the conductivity mechanism: from hopping to mixed hopping and fluid-like behavior.

References

[1] W.F. Kuhs, R. Nitsche, K. Scheunemann, Mater. Res. Bull. 14 (1979) 241–248.
[2] W.F. Kuhs, R. Nitsche, K. Scheunemann, Mater. Res. Bull. 11 (1976) 1115–1124.
[3] S. Fiechter, J. Eckstein, R. Nitsche, J. Cryst. Growth 61 (1983) 275–283.
[4] M. Evain, E. Gaudin, F. Boucher, V. Petricek, F. Taulelle, Acta Cryst. B 54 (1998) 376–383.
[5] R. Belin, A. Zerouale, A. Pradel, M. Ribes, Solid State Ion. 143 (2001) 445–455.
[6] I.P. Studenyak, Gy.Sh. Kovac, A.S. Orlyukas, Ye.T. Kovacs, Akad. Nauk. Ser. Fiz. 56 (1992) 86.
[7] I. Girnyk, D. Kaynts, O. Krupych, I. Martunyuk-Lototska, R. Vlokh, Ukr. J. Phys. Opt. 4 (2003) 147–153.
[8] S. Fiechter, E. Gmelin, Thermochim. Acta 87 (1985) 319–334.
[9] R.B. Beeken, J.J. Garbe, N.R. Petersen, J. Phys. Chem. Solids 64 (2003) 1261–1264.
[10] D.I. Kaynts, I.P. Studenyak, I.I. Nebola, A.A. Horvat, Ukr. J. Phys. Opt. 3 (2002) 267–270.
[11] M. Kranjcec, I.P. Studenyak, Gy.S. Kovacs, I.D. Desnica-Frankovic, V.V. Panko, P.P. Guranich, V.Yu. Slivka, J. Phys. Chem. Solids 62 (2001) 665–672.
[12] M. Kranjcec, I.P. Studenyak, V.V. Bilanchuk, V.S. Dyordyay, V.V. Panko, J. Phys. Chem. Solids 65 (2004) 1015–1020.
[13] I.P. Studenyak, M. Kranjcec, Gy.S. Kovacs, V.V. Panko, I.D. Desnica, A.G. Slivka, P.P. Guranich, J. Phys. Chem. Solids 60 (1999) 1897–1904.
[14] I.P. Studenyak, V.O. Stefanovich, M. Kranjcec, D.I. Desnica, Yu.M. Azhnyuk, Gy.Sh. Kovacs, V.V. Panko, Solid State Ion. 95 (1997) 221–225.
[15] I.P. Studenyak, M. Kranjcec, G.S. Kovacs, I.D. Desnica-Frankovic, V.V. Panko, V.Yu. Slivka, Mater. Res. Bull. 36 (2001) 123–135.
[16] I.P. Studenyak, M. Kranjcec, Gy.Sh. Kovacs, V.V. Panko, V.V. Mitrovcij, O.A. Mikajlo, Mater. Sci. Eng. B 97 (2003) 34–38.
[17] I.P. Studenyak, M. Kranjcec, Gy.S. Kovacs, V.V. Panko, Yu.M. Azhniuk, I.D. Desnica, O.M. Borets, Yu.V. Voroshilov, Mater. Sci. Eng. B 52 (1998) 202–207.
[18] A. Gągor, A. Pietraszko, M. Drozd, M. Polomska, D. Kaynts, Mater. Sci. (2006), ArXiv: cond-mat/0507300, accepted for publication.
[19] V. Petricek, M. Dusek, JANA2000, Institute of Physics, Praha, 2000.
[20] W.L. Bond, Acta Cryst. 13 (1960) 814–818.
[21] L.G. Berry, Am. Mineral. 39 (1954) 504.
[22] S.R. Hall, J.M. Steward, Acta Cryst. B 29 (1973) 579–585.

[23] P. Coppens, X-ray Charge Densities and Chemical Bonding, Oxford University Press, Oxford, 1997.
[24] A. Haznar, A. Pietraszko, I.P. Studenyak, Solid State Ion. 119 (1999) 31–36.
[25] R. Bachmann, H. Shulz, Acta Cryst. A 40 (1984) 668–675.
[26] J.K. Burdett, O. Eisenstein, Inorg. Chem. 31 (1992) 1758–1762.
[27] E. Gaudin, F. Boucher, V. Petricek, F. Taulelle, M. Evain, Acta Cryst. B 56 (2000) 402–408.
[28] R. Belin, L. Aldon, A. Zerouale, C. Belin, M. Ribes, Solid State Sci. 3 (2001) 251–265.
[29] W.F. Kuhs, R. Nitsche, K. Scheunemann, Acta Cryst. B 34 (1978) 64–70.